AD_____

GRANT NUMBER DAMD17-98-1-8152

TITLE: Structure Elucidation of the Rho-GTPase Activating DH-Homology Domain

PRINCIPAL INVESTIGATOR: Behzad Aghazadeh

CONTRACTING ORGANIZATION: Sloan-Kettering Institute for Cancer Research
New York, New York 10021

REPORT DATE: June 1999

TYPE OF REPORT: Annual Summary

PREPARED FOR: Commanding General
U.S. Army Medical Research and Materiel Command
Fort Detrick, Maryland 21702-5012

REPORT DOCUMENTATION PAGE

Form Approved
OMB No. 0704-0188

1. AGENCY USE ONLY *(Leave blank)*	2. REPORT DATE	3. REPORT TYPE AND DATES COVERED
	June 1999	Annual Summary (1 Jun 98 – 31 May 99)

4. TITLE AND SUBTITLE
Structure Elucidation of the Rho-GTPase Activating DH-Homology Domain

5. FUNDING NUMBERS
DAMD17-98-1-8152

6. AUTHOR(S)
Behzad Aghazadeh

7. PERFORMING ORGANIZATION NAME(S) AND ADDRESS(ES)
Sloan-Kettering Institute for Cancer Research
New York, New York 10021

8. PERFORMING ORGANIZATION REPORT NUMBER

9. SPONSORING / MONITORING AGENCY NAME(S) AND ADDRESS(ES)
U.S. Army Medical Research and Materiel Command
Fort Detrick, Maryland 21702-5012

10. SPONSORING / MONITORING AGENCY REPORT NUMBER

11. SUPPLEMENTARY NOTES

12a. DISTRIBUTION / AVAILABILITY STATEMENT
Approved for Public Release; Distribution Unlimited

12b. DISTRIBUTION CODE

13. ABSTRACT *(Maximum 200 words)*

Guanine nucleotide exchange factors in the Dbl family activate Rho GTPases by accelerating dissociation of bound GDP, promoting acquisition of the GTP-bound state. Dbl proteins possess an approximately 200 residue catalytic Dbl-homology (DH) domain, that is arranged in tandem with a C-terminal pleckstrin homology (PH) domain in nearly all cases. Here we report the solution structure of the DH domain of human βPIX. The domain is composed of 11 α-helices that form a flattened, elongated bundle. The structure explains a large body of mutagenesis data, which, along with sequence comparisons, identify the GTPase interaction site as a surface formed by three conserved helices near the center of one face of the domain. Proximity of the site to the DH C-terminus suggests a means by which PH-ligand interactions may be coupled to DH-GTPase interactions to regulate signaling through the Dbl proteins *in vivo*.

14. SUBJECT TERMS
Breast Cancer Dbl homolgy domians, rho-GTPase signaling, metastasis, NMR structure determination

15. NUMBER OF PAGES
19

16. PRICE CODE

17. SECURITY CLASSIFICATION OF REPORT	18. SECURITY CLASSIFICATION OF THIS PAGE	19. SECURITY CLASSIFICATION OF ABSTRACT	20. LIMITATION OF ABSTRACT
Unclassified	Unclassified	Unclassified	Unlimited

FOREWORD

Opinions, interpretations, conclusions and recommendations are those of the author and are not necessarily endorsed by the U.S. Army.

____ Where copyrighted material is quoted, permission has been obtained to use such material.

____ Where material from documents designated for limited distribution is quoted, permission has been obtained to use the material.

____ Citations of commercial organizations and trade names in this report do not constitute an official Department of Army endorsement or approval of the products or services of these organizations.

____ In conducting research using animals, the investigator(s) adhered to the "Guide for the Care and Use of Laboratory Animals," prepared by the Committee on Care and use of Laboratory Animals of the Institute of Laboratory Resources, national Research Council (NIH Publication No. 86-23, Revised 1985).

____ For the protection of human subjects, the investigator(s) adhered to policies of applicable Federal Law 45 CFR 46.

B.A. In conducting research utilizing recombinant DNA technology, the investigator(s) adhered to current guidelines promulgated by the National Institutes of Health.

B.A. In the conduct of research utilizing recombinant DNA, the investigator(s) adhered to the NIH Guidelines for Research Involving Recombinant DNA Molecules.

____ In the conduct of research involving hazardous organisms, the investigator(s) adhered to the CDC-NIH Guide for Biosafety in Microbiological and Biomedical Laboratories.

B.A. 6/30/99

PI - Signature Date

Table of Contents

5. Introduction

The Rho family GTPases Rho, Rac and Cdc42 regulate a diverse array of cellular processes such as regulation of the actin cytoskeleton, gene expression and cell cycle progression. Not surprisingly, aberrant Rho signaling can contribute to many disease processes, including tumorigenesis, tumor metastasis and developmental disorders. Activation of Rho proteins, through release of bound GDP and subsequent binding of GTP, is catalyzed by guanine nucleotide exchange factors (GEFs) in the Dbl family. All members of this group of over 30 molecules, most of which were initially identified based on their oncogenic potential, share a sequence of approximately 200 residues, termed the Dbl-homology (DH) domain. In order to provide a molecular framework for understanding DH-mediated nucleotide exchange activity, specificity and regulation, we have determined the solution structure of the DH domain of human βPIX. Mutagenic studies of the DH domains of Dbl, the archetypal member of the Dbl family, and UNC-73, a Dbl protein regulating axon guidance in *C. elegans*, together with sequence alignments, identify the probable GTPase interaction site. Future research will be aimed at obtaining a molecular basis for the interaction of DH domains with Rho-GTPases.

6. Body

The Rho family GTPases Rho, Rac and Cdc42 regulate a diverse array of cellular processes including regulation of the actin cytoskeleton, gene expression and cell cycle progression, and aberrant Rho signaling can contribute to many disease processes, including tumorigenesis, tumor metastasis and developmental disorders.

Activation of Rho-GTPases has been linked to the Dbl homology (DH) domain which was first discovered in the diffuse-B-cell lymphoma in 1985 and subsequently in over 30 molecules (mostly in assays identifying oncogenes) sharing this common domain of approximately 200 residues. Although a vast array of biochemical data exists, the 3-dimensional structure had yet to be elucidated in order to explain this data, including issues relating to activity toward GTPases specificity and mutangenesis rendering many of these molecules oncogenic.

We have determined the solution structure of the DH domain of βPix, a recently identified member of this family. Furthermore we were able to map the GTPase interaction site based on structure-based amino acid sequence alignment. Knowledge of the structure also guided our mutagenesis studies which led to the biochemical verification of the active site and the identification of key residues involved in GEF function.

Structure determination of the DH domain by NMR spectroscopy posed a significant challenge. There have been to date no NMR structures of molecules of such relatively large size (24kDa)

without prior knowledge of the X-ray structure. Several factors including the size and helical nature of the molecule complicated every step significantly.

In order to overcome the difficulties, we devised a strategy involving state-of-the-art labeling schemes to obtain both chemical shift and NOE assignments from NMR experiments especially designed for these labeling patterns. This was the first time the full scope of the latest biochemical and spectroscopic advances were employed in determining an unknown structure. Furthermore, we had to employ the latest structure calculation protocols (CNS) together with an automated NOE assignment program (ARIA) in order to obtain converging structures and be able to further refine the structure. The final structure is of high quality with a root-mean-square-deviation for an ensemble of 20 structures of 0.79 Å for the helices only and 1.09 Å for the structured portion of the molecule.

The tandem occurence of the DH domain with pleckstrin homology (PH) domains suggests that the Dbl family PH domains may also play a more specific role in regulating GEF activity. We do not however observe any structural interactions between these domains of βPix in solution.

Structure and sequence homolgy directed mutagenesis on a variety of DH constructs enabled us to identify regions of the molecule involved in GTPase nucleotide exchange. Both NMR spectroscopic and biochemical nucleotide exchange assays were performed.

Based on this information, we believe to be able to explain the low exchange activity of βPix toward GTPases. Several residues in the proposed GTPase interaction surface that are conserved in the DH family are not conserved in βPix. Future focus will be directed to determine the relative significance of these residues in mediating nucleotide exchange.

Knowledge of the structure of the DH domain will also help us in investigating the regulation of these molecules, the loss of which renders these molecules oncogenic.

7. Appendix

Research accomplishments

- The solution structure of the βPix DH domain has been determined by multi-dimensional NMR spectroscopy.
- The structure forms an elongated bundle of α-helices, bringing together several regions of high sequence conservation.
- The probable GTPase interaction site has been determined to lie on one face of the protein defined by three conserved helices.

Publications

Aghazadeh, B., Zhu, K., Kubiseski, T.J., Liu, G.A., Pawson, T., Zheng, Y. & Rosen, M.K. Structure and Mutagenesis of the Dbl Homology Domain. *Nature Structural Biology* **5** (12), 1098-1107 (1998).

Structure and mutagenesis of the Dbl homology domain

Behzad Aghazadeh[1,2], Kejin Zhu[4], Terrance J. Kubiseski[5], Grace A. Liu[1], Tony Pawson[5], Yi Zheng[4] and Michael K. Rosen[1,3]

Guanine nucleotide exchange factors in the Dbl family activate Rho GTPases by accelerating dissociation of bound GDP, promoting acquisition of the GTP-bound state. Dbl proteins possess a ~200 residue catalytic Dbl-homology (DH) domain, that is arranged in tandem with a C-terminal pleckstrin homology (PH) domain in nearly all cases. Here we report the solution structure of the DH domain of human PAK-interacting exchange protein (βPIX). The domain is composed of 11 α-helices that form a flattened, elongated bundle. The structure explains a large body of mutagenesis data, which, along with sequence comparisons, identify the GTPase interaction site as a surface formed by three conserved helices near the center of one face of the domain. Proximity of the site to the DH C-terminus suggests a means by which PH-ligand interactions may be coupled to DH-GTPase interactions to regulate signaling through the Dbl proteins *in vivo*.

The Rho family GTPases Rho, Rac and Cdc42 regulate a diverse array of cellular processes[1]. Best understood as regulators of the actin cytoskeleton, each member of the family is capable of inducing distinct actin-based structures upon activation. Cdc42 can induce formation of fillipodia and focal complexes[2,3]; Rac, formation of lamellipodia and focal complexes[3,4]; and Rho, actin stress fibers and focal adhesions[5]. Rho proteins also regulate gene expression[6–10] and cell cycle progression[6], implicating them in control of cell growth. Not surprisingly, aberrant Rho signaling can contribute to many disease processes, including tumorigenesis[11], tumor metastasis[12] and developmental disorders[13,14].

Like all members of the Ras superfamily, the Rho proteins cycle between active GTP-bound and inactive GDP-bound conformational states. In this way, they function as molecular switches in signaling pathways, controlling information transfer from cell surface receptors to intracellular machinery[15]. The nucleotide binding and hydrolysis cycle is intrinsically slow, and is regulated *in vivo* by a variety of proteins that serve to accelerate or block different steps in the process[16,17]. Activation of Rho proteins, through release of bound GDP and subsequent binding of GTP, is catalyzed by guanine nucleotide exchange factors (GEFs) in the Dbl family[18]. All members of this group of over 30 molecules share a sequence of ~200 residues, termed the Dbl-homology (DH) domain (Fig. 1)[19–21]. While biochemical studies have revealed that GEF activity resides in the DH domain, they have also found wide variation in the GTPase binding and catalytic behavior of individual Dbl proteins. Some family members have catalytic activity only toward a single GTPase, such as the Cdc42 specific FGD1[22] and the Rac specific UNC-73B[23]. Others act on a broader range of targets, such as Dbl[20] and Ost[24] which both activate Cdc42 and Rho. Still others (such as Ect-2) bind GTPases (Rho and Rac) but have no detectable GEF activity toward currently known Rho proteins[25]. Lastly, and most unusual from a mechanistic perspective, some DH domains are GEFs for certain GTPases, but bind others without causing nucleotide exchange. These include Lfc, which activates Rho but binds Rac as well[26], and Ost which activates Cdc42 and Rho but binds Rac in a GTP-dependent manner[24]. This range of behavior has led to speculation that DH domains may not function exclusively as GEFs in the cell, but could also play roles in recruiting GTPases to specific locations or to specific molecular targets[26].

Mechanistic details of DH-mediated GEF catalysis are poorly understood. However, it is generally believed that DH domains will function analogously to other, better characterized exchange factors such as RCC1[27] and the Cdc25 domain, which act on Ran and Ras respectively. In these cases, detailed kinetic and thermodynamic analyses have demonstrated that GEF binding decreases GTPase nucleotide affinity by several orders of magnitude, principally by effecting an increase in dissociation rate. GEF complexation thus allows nucleotide state to equilibrate with conditions in the cell; as cellular GTP concentration is typically 10-fold higher than GDP concentration (10^{-4} M *versus* 10^{-5} M), equilibration results in GTPase activation[27]. The recently reported structures of the Cdc25 and SEC7 GEF domains bound to their GTPase substrates Ras and Arf respectively, have demonstrated that these effects result from a complex series of interactions, involving large rearrangements of the switch I and II regions of the GTPase and specific interactions with the phosphate and Mg^{2+} binding sites. It is not yet clear if the principles that have emerged from these structures will be generalizable to the actions of DH domains toward Rho family GTPases.

In virtually all Dbl proteins, the DH domain is immediately followed in sequence by a ~100 residue pleckstrin homology (PH) domain, a widely distributed signaling module often involved in intracellular membrane targeting[28,29]. A variety of studies indicate that the PH domain is necessary for proper intracellular localization and function of Dbl proteins. In this sense PH domain interactions in Rho signaling pathways could

[1]Cellular Biochemistry and Biophysics Program, Memorial Sloan-Kettering Cancer Center, 1275 York Avenue, New York, New York 10021, USA. [2]Graduate Program in Physiology and Biophysics, Cornell University Graduate School of Medical Sciences, New York, New York 10021, USA. [3]Graduate Program in Biochemistry and Structural Biology, Cornell University Graduate School of Medical Sciences, New York, New York 10021, USA. [4]Department of Biochemistry, University of Tennessee, Memphis, Tennessee 38163, USA. [5]Programme in Molecular Biology and Cancer, Samuel Lunenfeld Research Institute, Mount Sinai Hospital, Toronto, Ontario M5G 1X5, Canada.

Correspondence should be addressed to M.K.R. *email: rosen@mrnmr1.ski.mskcc.org*

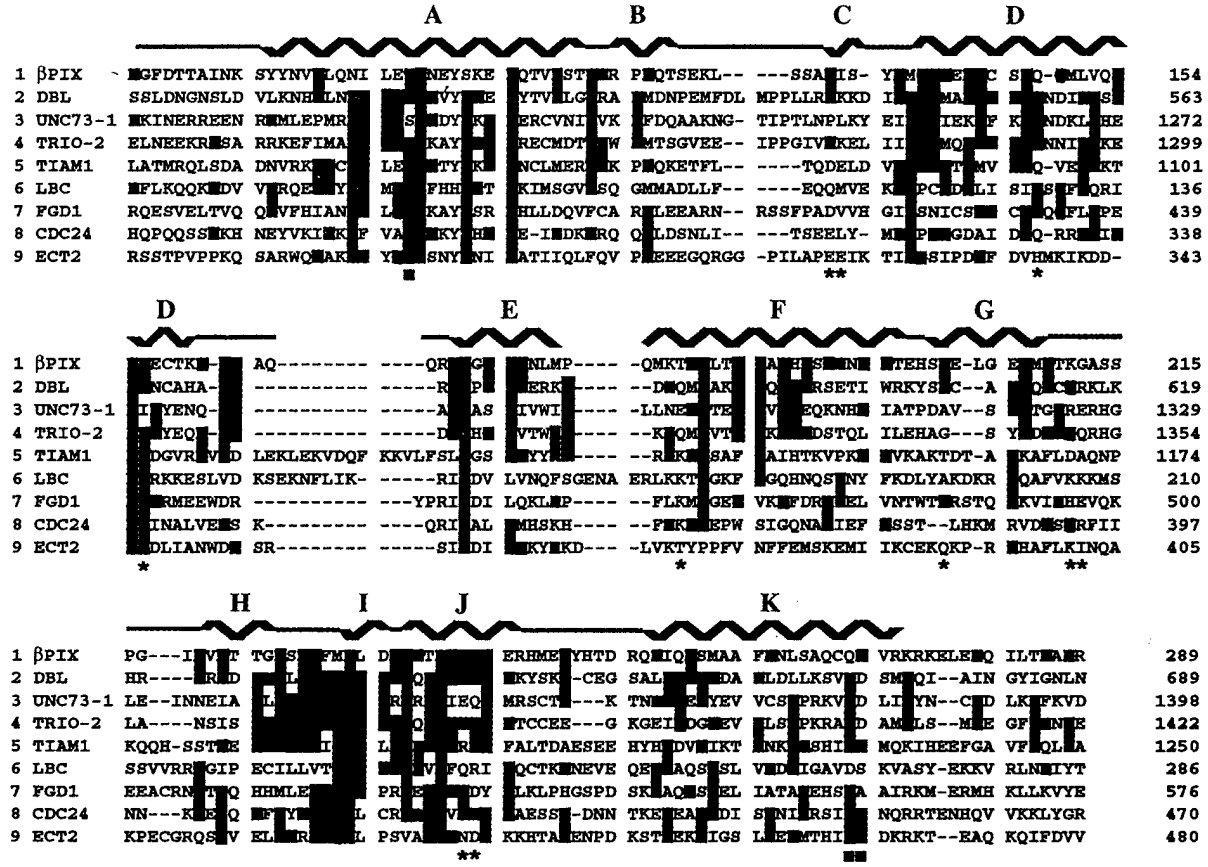

Fig. 1 Structure-based amino acid sequence alignment (manually modified Clustal) of selected Dbl homology domains. Residues appearing in three or more sequences are boxed in red. Consensus secondary structure of the βPIX DH domain as determined by Procheck-NMR[79] is shown above the sequence. Residues whose mutation resulted in inactivation of Dbl or UNC-73 are indicated below the alignment by a ■. Those whose mutation had no effect on the GEF activity of Dbl are indicated by a *.

function analogously to SH2 and SH3 domain interactions in the Ras pathway, to activate GEFs by recruiting them to membranes, where the prenylated GTPases reside[28]. However, the stereotypical pairing of DH with PH suggests that the Dbl family PH domains may also play a more specific role in regulating GEF activity. This could include direct contribution of binding or catalytic residues, allosteric modulation of catalytic activity, recruitment of additional regulatory factors or precise positioning with respect to GTPases following membrane targeting.

In order to provide a molecular framework for understanding DH-mediated nucleotide exchange activity, specificity and regulation, we have determined the solution structure of the DH domain of human βPIX (also referred to as p85^{Cool-1}, ref. 30) a recently reported member of the Dbl family[31]. The structure forms an elongated bundle of α-helices, bringing together several regions of high sequence conservation. Mutagenic studies of the DH domains of Dbl, the archetypal member of the Dbl family, and UNC-73, a Dbl protein regulating axon guidance in *C. elegans*[23], together with sequence alignments, identify the probable GTPase interaction site as a flat surface on one face of the protein defined by three conserved helices. Although the DH and PH domains of a βPIX tandem construct do not interact in solution, proximity of the GTPase contact site to the DH C-terminus suggests that such an interaction could occur in other Dbl proteins having complementary DH and PH surfaces.

Structure determination

βPIX possesses a unique splice variant in which the 357 amino acids C-terminal to Lys 289, including the PH domain and much of the interdomain linker, have been replaced with ~25 residues of apparently random sequence (S. Bagrodia and R. A. Cerione, unpublished results). The construct used in the structure determination was based on this variant, and spans residues 82–289 of the protein.

Structure determination of the DH domain by NMR spectroscopy represented a significant challenge. The relatively large size of the protein (24,000 M_r) coupled with its elongated shape (see below) resulted in short T2 relaxation times and correspondingly low sensitivity in many experiments typically used to make chemical shift assignments. Moreover, the paucity of aromatic residues (six phenylalanines, nine tyrosines, 0 tryptophans) and overabundance of leucine residues (29, versus nine valines and eight isoleucines), exacerbated the already poor chemical shift dispersion resulting from the helical nature of the protein.

In order to overcome these difficulties, extensive use was made of selective deuteration strategies to obtain both chemical shift and NOE assignments. Nearly complete backbone ^{1}HN, ^{15}N, ^{13}CO, ^{13}Cα (98%) and ^{13}Cβ (98%) sequential assignments were achieved through analyses of ^{2}H/^{15}N/^{13}C-labeled samples (see the Methods; note that all amide positions in deuterated samples are fully protonated due to solvent exchange during purification).

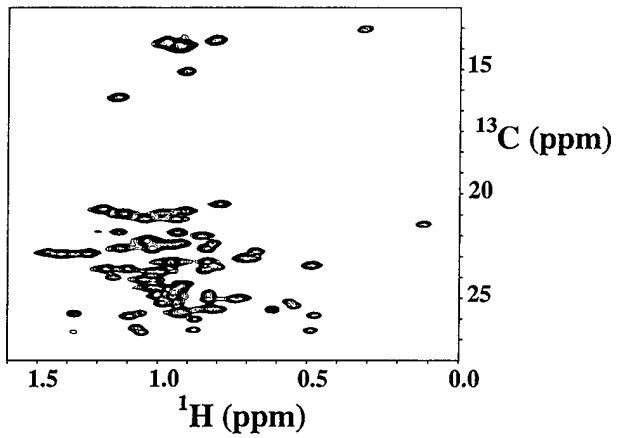

Fig. 2 Methyl region of a constant time ^{1}H/^{13}C HSQC spectrum of the βPIX DH domain recorded at 38 °C on the selectively methyl/aromatic protonated sample described in the text.

Many side chain assignments were made through a combination of HCC- and CCC-TOCSY-NNH[32] experiments recorded on a ^{2}H(50%)/^{15}N/^{13}C-labeled sample, and HCCH-TOCSY[33] experiments recorded on ^{15}N/^{13}C samples. However, due to poor transfer efficiency and extensive methyl chemical shift degeneracy (Fig. 2), these spectra yielded very few assignments of the critical leucine and isoleucine methyl groups necessary to define the hydrophobic core of the protein.

Key to the structure determination process was a sample labeled uniformly with ^{15}N, and with ^{1}H/^{13}C at the methyl groups of Val, Leu and Ile (δ only) residues, ^{1}H/^{12}C at Phe and Tyr residues, and ^{2}H/^{13}C at all other carbon sites[34–38]. Methyl optimized HCC- and CCC-TOCSY-NNH spectra[39] recorded on this sample provided rapid, unambiguous assignments of all valine, leucine and isoleucine (δ only) methyl proton and carbon chemical shifts. In addition, the long relaxation times afforded by high level deuteration enabled acquisition of high-sensitivity and high-resolution homonuclear ^{1}H-TOCSY experiments to obtain complete assignments of aromatic ring protons, which were then connected to the backbone using traditional NOE-based methods[40].

The selective methyl/aromatic labeled sample was also critical to determination of the global fold of the DH domain. Specifically, the narrow aliphatic proton and carbon chemical shift ranges (1.4 p.p.m. and 15 p.p.m. respectively) afforded by the labeling pattern facilitated acquisition of a series of high resolution and high sensitivity NOESY spectra to obtain long-range methyl and aromatic NOEs defining the hydrophobic core. Thus a homonuclear 2D NOESY spectrum afforded 24 aromatic-aromatic and 11 aromatic-methyl NOE assignments, and a 4D ^{13}C-^{13}C spectrum afforded 81 methyl-methyl NOE assignments based entirely on chemical shifts. Zwahlen *et al.* have recently described a 3D constant time ^{13}C-NOESY pulse sequence specifically designed for identification of methyl-methyl NOEs in selectively methyl protonated samples[41]. A modified version of this sequence (M.K.R., unpublished), in which both methyl ^{1}H and ^{13}C chemical shifts are recorded prior to NOESY transfer (the latter in constant-time mode), followed by acquisition of all protons in the direct dimension was particularly useful in assignment of methyl-aromatic NOEs in the DH domain. High resolution in all dimensions of the spectrum enabled assignment of 101 crosspeaks involving 36 residues. In total, the methyl/aromatic sample provided an initial set of 261 restraints. These, together with 665 amide and 65 additional aliphatic short- and medium-range restraints (protons separated by 0–1 or 2–5 residues respectively), 100 hydrogen bond restraints (assigned based on slowly exchanging amides in CSI-defined[42] helical regions), 116 ϕ and 116 ψ restraints (see the Methods), were sufficient to define the global fold of the domain. Calculations performed without aromatic NOE restraints did not yield convergent structures.

Following determination of the global fold, additional NOEs were assigned in an iterative fashion using the program ARIA[43]. The final ensemble of 20 lowest energy structures is based on a total of 2,507 NOE-based restraints, 130 hydrogen bond restraints, 232 backbone dihedral restraints and 52 side chain dihedral restraints. Residues 81–92 and 274–289 show no long range NOEs and exhibit intermediate (81–92, 274–280) or fast (281–289) exchange, indicating they do not have a discreet structure in the protein. Coordinate precision (defined as the root-mean-square (r.m.s.) deviation from the average structure) for residues 93–273 in the 20 final conformers is 1.07 Å for backbone atoms, and 1.64 Å for all heavy atoms. In regions of secondary structure these values are 0.82 Å and 1.26 Å respectively.

DH domain structure

The DH domain is a flattened, elongated bundle of 11 α-helices (approximate dimensions 60 Å × 30 Å × 20 Å), designated A–K in Fig. 4. Seven of these can be grouped into five segments that align approximately along the long axis of the protein. Segment 1 consists of helix A, segment 2 of helix D, segment 3 of helices E, F and G, segment 4 of helices I and J, and segment 5 of helix K. Segments 1–4 are organized in an up-and-down bundle, roughly around the corners of a parallelogram (Fig. 4*b*). Helix K packs at one side of this polygon in a groove formed by helices E/F and J, resulting in an overall trapezoidal shape when viewed down the long axis of the protein (Fig. 4*b*). Segments 1 and 4 are the most highly conserved regions of the protein, and along with helix K form one elongated face of the structure. The opposite face, formed by segments 2 and 3, is much less conserved, with segment 3 in particular showing large variability in residue composition and length of the E-F linker. The structure shows only minimal similarity to proteins in the structural database (maximum DALI[44] Z-score = 3.4), and is unrelated to the exchange

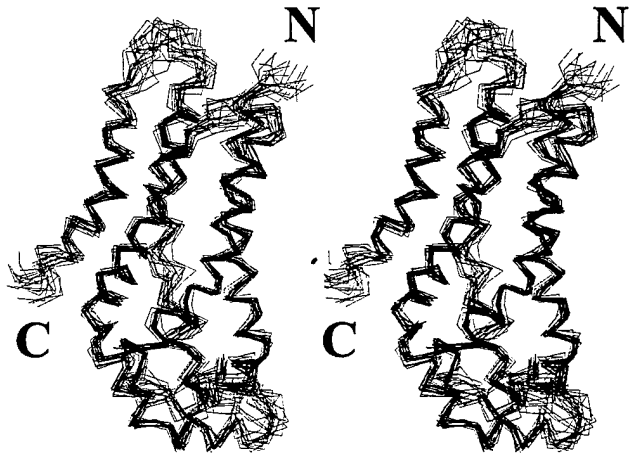

Fig. 3 Stereo view of the backbone (N, Cα, C') of 20 final superimposed structures of the βPIX DH domain. Residues 81–92 and 274–289 of the construct are disordered in solution, not defined by the NMR data, and have been removed for clarity.

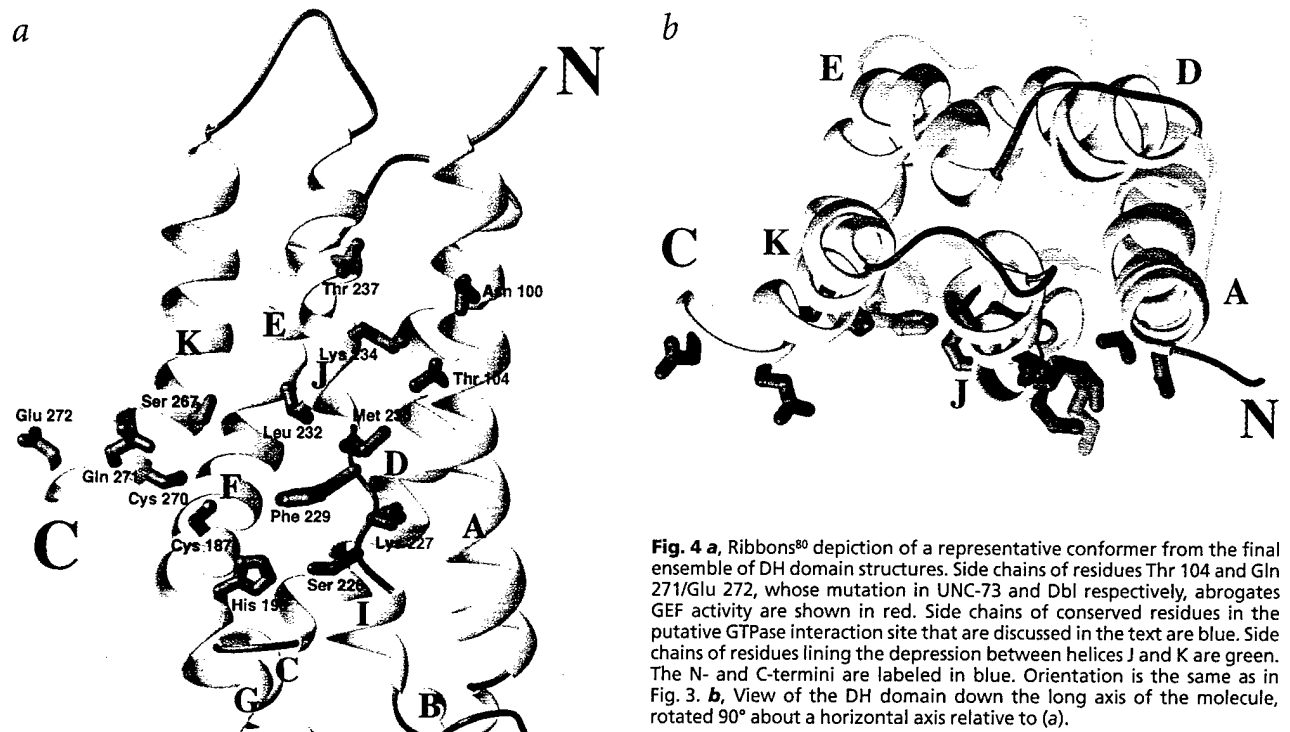

Fig. 4 ***a***, Ribbons[80] depiction of a representative conformer from the final ensemble of DH domain structures. Side chains of residues Thr 104 and Gln 271/Glu 272, whose mutation in UNC-73 and Dbl respectively, abrogates GEF activity are shown in red. Side chains of conserved residues in the putative GTPase interaction site that are discussed in the text are blue. Side chains of residues lining the depression between helices J and K are green. The N- and C-termini are labeled in blue. Orientation is the same as in Fig. 3. ***b***, View of the DH domain down the long axis of the molecule, rotated 90° about a horizontal axis relative to (*a*).

factors for other small GTPases, including MSS4[45], SEC7[46,47], RCC1[48] and SOS[49].

DH-PH Relationship

In order to identify potential contacts between the DH and PH domains in βPIX, $^{1}H/^{15}N$ correlation TROSY[50] spectra of $^{2}H/^{15}N$-labeled DH and DH-PH (residues 82 to 406) constructs were obtained. At 38 °C, DH resonances in the two data sets (repeated on two separate samples each) showed only small deviations ($\delta = ((\Delta^{1}H \text{ p.p.m.})^2 + (\Delta\ ^{15}N \text{ p.p.m./9.8})^2)^{1/2}) < 0.03$ p.p.m.) for all amides in the structured portion of the domain. A pattern of slightly larger changes (0.02 p.p.m. $< \delta <$ 0.03 p.p.m.) was observed for residues near the F-G junction, which is adjacent to the DH C-terminus in the structure. However, the magnitude of these differences is clearly not indicative of a packed interface between the DH domain and residues of the PH or linker regions. This notion is further supported by the observation that in $^{1}H/^{15}N$ HSQC spectra of the DH-PH construct, DH resonances are uniformly broader and weaker than those of the PH domain and linker. Thus, in the absence of additional factors (such as a GTPase) the DH and PH domains of βPIX are not packed together into a single unit, but rather behave more like two independent structural domains in solution.

Mutagenesis

The structure explains a large body of mutagenesis data obtained by ourselves and others on a variety of DH domains. Many of the described inactivating mutations clearly act through disruption of structure. The disease-causing mutation in the faciogenital dysplasia 1 (FGD1) gene results in a frameshift at codon 465, and premature chain termination four residues later[13]. The site of mutation corresponds to Lys 180 in βPIX, which lies at the predicted N-terminus of helix E. Thus, the FGD1 mutant is a severely truncated protein that is unable to fold. Similarly, the Dbl-inactivating deletions of residues 505–518 and 664–670 (βPIX residues 102–115 and 261–267) reported by Hart *et al.* would eliminate portions of the A and K helices respectively, again destabilizing the fold of the protein[20]. Mutation of Leu 213 to Gln in the Vav oncogene eliminates both transforming potential and the ability of the protein to activate PAK kinase through Rac1[51]. This residue corresponds to the highly conserved Leu 112 in βPIX, which is located on the buried face of helix A, and makes numerous contacts in the protein hydrophobic core to sidechains in helices D and I. Replacement with a hydrophilic side chain would likely disrupt the core and prevent folding of the domain.

Other mutations appear to have more direct effects on GTPase binding or GEF catalysis, as they involve conserved residues that are solvent exposed in the structure. We have previously reported that an inactivating allele of UNC-73, a gene necessary for neuronal pathfinding in *C. elegans*, contains a mutation in codon 1216 that changes Ser to Phe in the DH domain of the protein[23]. The mutation also blocks the ability of purified recombinant UNC-73 expressed in insect cells to activate Rac1 *in vitro*. This residue (Thr 104 in βPIX) is either Ser or Thr in virtually all known DH domains and is located on the exposed face of helix A, adjacent to helix J (Figs. 4, 6). Continued analyses of UNC-73 have revealed that mutation of Ser 1216 to Thr has no effect on the ability of the recombinant protein to catalyze nucleotide exchange on Rac (Fig. 5*a*). However, mutation to either Ala or Glu resulted in elimination of any significant activity at the protein concentrations tested. These data indicate that the Ser/Thr at the position corresponding to Thr 104 in βPIX, and in particular the hydroxyl group of this residue, is likely to mediate interactions with Rac1 that are necessary for GEF catalysis.

To further delineate regions of DH-GTPase interaction, we have also prepared a battery of mutations in the DH domain of

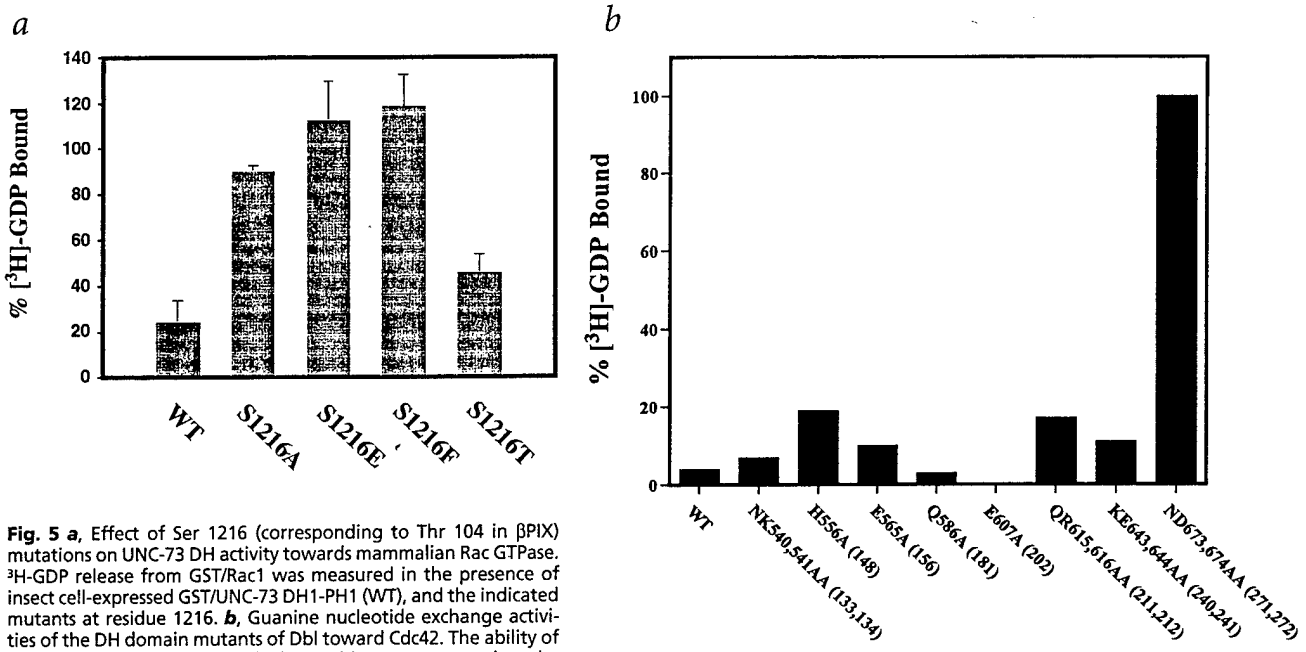

Fig. 5 ***a***, Effect of Ser 1216 (corresponding to Thr 104 in βPIX) mutations on UNC-73 DH activity towards mammalian Rac GTPase. ^{3}H-GDP release from GST/Rac1 was measured in the presence of insect cell-expressed GST/UNC-73 DH1-PH1 (WT), and the indicated mutants at residue 1216. ***b***, Guanine nucleotide exchange activities of the DH domain mutants of Dbl toward Cdc42. The ability of the insect cell-expressed, purified GST-Dbl mutants to catalyze the release of ^{3}H-GDP from the GTPase was measured. Similar results were obtained for the GEF activity of these mutants toward Rho. The experiment shown is representative of at least two independent assays using proteins from different preparations. Both bar graphs represent the amount of ^{3}H-GDP bound to the GTPase after 20 min (Rac1/UNC-73) or 5 min (Cdc42/Dbl) in the presence of the exchange factor.

Dbl. Recombinant proteins were expressed in baculovirus infected insect cells, purified and assayed for GEF activity toward Cdc42 and Rho. Essentially identical results were obtained for the two GTPases, and only data on the former are described here. Most of the mutants show GEF activity identical to wild type (Fig. 5*b*). Thus, double mutants N540A/K541A, Q615A/R616A and K643A/E644A, which correspond to changes of N133/I134, K211/G212 and K240/E241 in βPIX are fully active. Results similar to the last of these have also been reported in an analysis of the *S. cerivisiae* Cdc24 gene. There, mutation of Lys 442 to Glu or Glu 423 to Lys (βPIX, K240E or E241K) resulted in no observable phenotype, in contrast to the severe defects in budding observed on disruption of the gene[52]. The three double mutants are located in solvent exposed regions of helix C, the G-H loop, and C-terminal end of helix J respectively, and indicate that these regions do not play a significant role in mediating GEF catalysis. Single residue changes of H556A, E565A, Q586A and E607A, corresponding to Q148A, E156A, T181A and E202A, in βPIX are also without effect on GEF activity toward Cdc42 or RhoA. These changes involve exposed residues at the center and C-terminus of helix D, near the N-terminus of helix F and at the N-terminus of helix G respectively, indicating these regions, too, are uninvolved in nucleotide exchange catalysis.

One double mutant, N673A/D674A, did show severely impaired GEF activity (Fig. 5*b*). These residues correspond to Gln 271 and Glu 272 in βPIX, which are located on the solvent exposed face of helix K at its C-terminal end (Figs 4, 6). The first is highly conserved throughout the Dbl family, being an Asn in >75% of the reported sequences. Notably, βPIX is an exception to this trend, having a Gln at this position. The second residue, Asp 674, is either an Asp or a Glu in the majority of DH domains. The high conservation of these exposed residues and loss of activity on mutation suggests that either or both play a direct role in GEF activity of Dbl toward Cdc42 and RhoA.

GTPase interaction site

The mutagenesis data above have identified two sites on the solvent exposed surface of the A and K helices that are likely to mediate DH domain interactions with GTPases during GEF catalysis. They have also excluded sites on the C, D, F and G helices, the G-H loop and the C-terminus of helix J from direct participation in the nucleotide exchange process. In order to identify other potential DH domain-GTPase contact sites we analyzed patterns of surface residue conservation throughout the Dbl family. A surface of the DH domain, colored according to degree of conservation among the proteins listed in Fig. 1, is shown in Fig. 6. There is pronounced clustering of conserved residues on one of the long faces of the protein, composed of segments 1, 4 and 5. The most conserved region lies between Thr 104 and Q271/E272, the contact residues identified through mutagenesis. On this basis, we conclude that the surface of the DH domain bounded by the A and K helices horizontally in Fig. 4 and spanning approximately the middle third of the molecule vertically is likely to be the GTPase contact site.

The central portion of the interaction site consists of solvent exposed side chains in the I-J loop and helix J. Residues at positions 227, 230, 234 and 237 are all directed into solvent, and are conserved across the Dbl family. The first three of these are hydrophilic in character, with 227 being Lys, 230 Gln and 234 Lys or Arg in most DH domains. It is notable that position 230 is particularly highly conserved, yet is Met in βPIX. Residue 237 is hydrophobic, being Leu or Val in most DH domains, but again is distinct in βPIX, which has a Thr at this position. These differences, along with that at residue 271 mentioned above, may

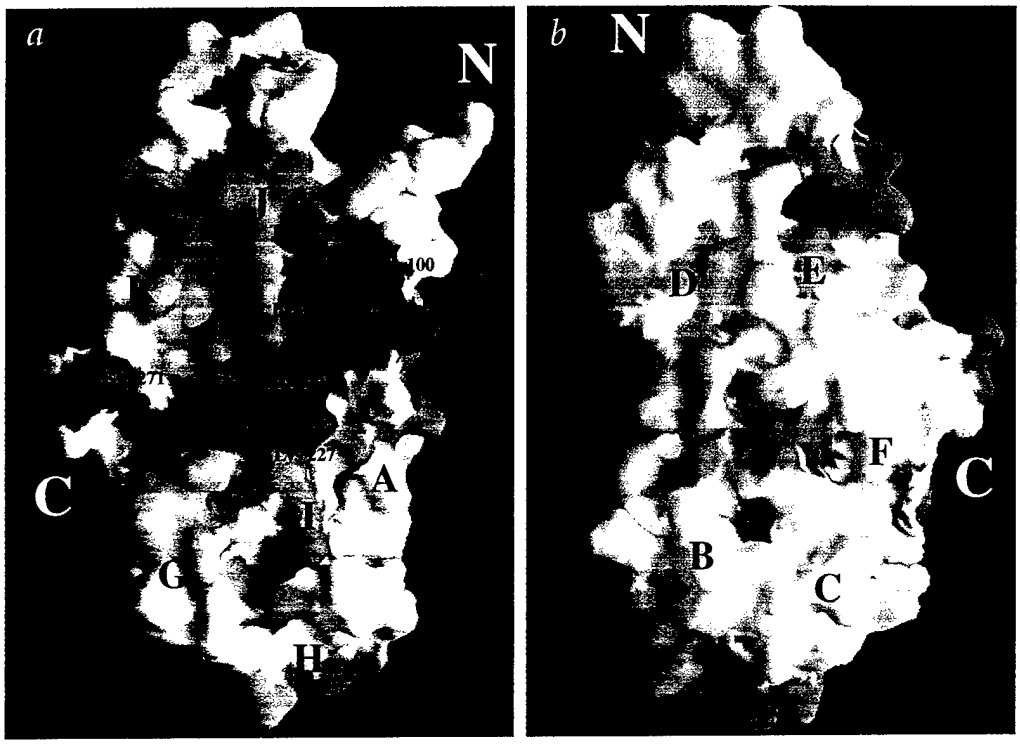

Fig. 6 ***a***, Molecular surface of the DH domain oriented as in Fig. 3. Residues are color coded according to sequence conservation among the proteins listed in Fig. 1. The color scale varies from white, representing conservation in three or less Dbl domains, to red, representing conservation in all nine domains. Helices are labeled in black, and the N- and C-termini are labeled in white ***b***, View following rotation of the surface by 180° about a vertical axis. Figures were created using the program GRASP[81].

account for the low GEF activity of βPIX observed by ourselves and others (B.A., M.K.R., unpublished results; refs 30, 31). The break between helices I and J occurs near one end of the conserved site and appears to be caused by Pro 228. This residue, whose side chain is completely buried, is nearly invariant in DH domains. The structure imparted by the break in the helices may thus be important in organization of the GEF active site. Structure in the J helix may also be important for catalysis based on observations that in Dbl, Cdc24 and Vav, the conservative mutation of residues corresponding to 237–243 in βPIX (LLLKELL in Dbl) to IIIRDII abolishes GEF activity[20,51,53]. Residues Lys 240 and Glu 241 (βPIX numbering) in this sequence can be mutated in Dbl without decreasing GEF activity. Thus, since substitution of Leu with Ile would not be expected to grossly destabilize DH structure, the inhibitory effects of this mutation suggest that GEF catalysis may be particularly sensitive to the structure of the J helix.

The conserved residues in helix J are flanked on one side by exposed side chains in helix A. Many of these are also conserved, and the majority again are hydrophilic. Residues 100 and 104 are Glu and Thr/Ser in most DH domains. Their side chains contact those at positions 237, 234 and 230, forming a continuous region of conserved surface. Beneath this surface, a nearly invariant internal salt bridge involving βPIX residues Glu 105 and Arg 231 serves to stabilize packing between the A and J helices, and maintain the structure of the active site.

Helix K packs against the opposite side of helix J. While the majority of this C-terminal segment has relatively variable sequence, position 271 is Asn in most cases. This residue is separated from conserved residues 227 and 230 by a shallow depression between the N-terminus of helix J and the C-terminus of helix K. This feature is lined by the side chains of Ser 226, Phe 229, Leu 232, Ser 267, Cys 270, Cys 187 and His 190. Although polar in βPIX, sequence alignment shows that the depression will be highly hydrophobic in most other DH domains (Fig. 1). In particular, side chains at positions 226, 229, 232, 267 and 270 are aliphatic or aromatic in nearly all cases. The active sites of the SEC7 and Cdc25 GEF domains both contain, in addition to hydrophilic residues, important hydrophobic clusters that make key contacts to residues in the switch II regions of their GTPase targets. The depression between helices J and K is the only comparable region on the conserved face of the DH domain. Thus, it is possible that this region of the DH domain may make similarly important contacts to hydrophobic portions of the Rho GTPases during GEF catalysis.

The exposed side chains of helices A, I/J and K form a slightly convex, largely hydrophilic surface with an adjacent depression that is hydrophobic in most DH domains. This region is the likely GEF active site of the DH domain. Importantly, the site is located immediately adjacent to the C-terminus of the folded structure. Thus, the sites of PH attachment and GTPase binding are proximal. This suggests a means of communication between the two domains that could be used to modulate GTPase interactions and GEF activity *in vivo*.

Functional implications

The nearly universal pairing of DH with PH suggests that the activities of the two domains may be functionally coupled. Evidence for this idea has been provided in analyses of the DH-PH tandem of SOS. Structures of the PH domains from human and mouse SOS contain an additional N-terminal α-helix not found in other PH domains[54,55]. This element, which appears to be part of the DH-PH linker in the full length protein, packs very near the phospholipid binding site of the PH domain. This observation has led to suggestions that in full length SOS, the DH and PH domains may contact each other in a manner modulated by lipid binding, and that this modulation could play a role in regulating GEF activity[54,55]. Interdomain regulation is supported by the discovery of Nimnual *et al.* that expression of the SOS DH domain alone in COS-1 cells results in activation of Rac, while the DH-PH tandem has this effect only when coexpressed with acti-

Table 1 Structural statistics[1]

Restraints for structure calculation	
Total restraints used	2,847
Total NOE restraints	2,507
Total Unambiguous Restraints	2,263
Intraresidue	1,212
Sequential	566
Medium range	284
Long range	201
Total Ambiguous Restraints	244
Hydrogen bond restraints	130
Dihedrals ϕ	116
Dihedrals ψ	116
Dihedrals χ (Thr, Leu, Val, Ile)	52
Statistics for structure calculations	
R.m.s.d. from experimental restraints[2]	
Distances (Å)	0.019 Å ± 0.002
Angles (°)	0.29° ± 0.17
Final Energies (kcal mol^{-1})	
E_{total}	474 ± 28
E_{bonds}	17 ± 4
E_{angles}	148 ± 12
E_{vdW}	35 ± 3
E_{NOE}	47 ± 8
Coordinate precision[3]	
R.m.s.d. of Backbone Atoms (N, Cα, C')	
Helices	0.79 Å ± 0.12
Residues 13–193	1.09 Å ± 0.16
R.m.s.d. of all Heavy Atoms	
Helices	1.24
Residues 13–193	1.65
Procheck	
Residues in most favored region	
Helices	86%
Residues 13–193	79%
Residues in additional allowed region	
Helices	13%
Residues 13–193	17%
Residues in generously allowed region	
Helices	0.6%
Residues 13–193	2.3%
Residues in disallowed region	
Helices	0.8%
Residues 13–193	1.8%

[1]The final values for the force constants employed for the various terms in the target function employed for simulated annealing are as follows: 5 kcal mol^{-1}Å^{-4} for the quartic van der Waals repulsion term (with van der Waals radii set to 0.78 times their value defined in the paramallhdg-pro parameter set), 50 kcal mol^{-1}Å^{-2} for the experimental distance restraints, 200 kcal mol^{-1}rad^{-2} for the experimental torsion angle restraints.[2]None of the final structures have distance restraint violations greater than 0.3 Å or dihedral violations greater than 5°.
[3]Defined as average root-mean-squared difference for the stated residues between the final 20 structures and the average coordinates.

vated Ras[56] that is capable of stimulating phosphatidyl inositol 3'-kinase (PI3'K). On this basis it was postulated that binding of the lipid product of PI3'K, phosphatidylinositol-3,4,5-triphosphate, to the SOS PH domain may enhance DH domain GEF activity. Such phenomena, however, are not universal. The DH and PH domains of βPIX clearly act as independent units in a tandem construct in solution. It is possible that the behavior observed here is specific to this system, since the βPIX splice variant mentioned above is the only known Dbl protein lacking a PH domain. But data on other Dbl proteins suggest this is not so. For example, the Lbc DH domain alone can stimulate DNA synthesis and actin stress fiber formation[57]. Alternatively, while the transforming activity of the Lfc oncogene can be eliminated through removal of its PH domain, activity is retained when the domain is substituted by a prenylation sequence[58], indicating the PH domain plays either both inhibitory and targeting roles or simply the latter in mediating transformation. Thus, although the structural data presented here demonstrate the potential for DH-PH interactions in the tandem, realization of this potential evidently does not occur in all cases. In fact, these interactions themselves may be regulated, either by the additional domains in the molecule, or through binding of additional molecules. In this regard, it is interesting that βPIX has been found in a stable ternary complex with activated Cdc42 and PAK[30]. Structural and biochemical analyses of this complex may yield additional insights into the control of GEF activity *in vivo*.

Sequence alignments show that there are no completely invariant residues in the DH domain. Even residues in the GTPase interaction site show some variation across the family. This may reflect both the nature of nucleotide exchange catalysis and differences in activity and regulation of the Dbl family members. A fundamental feature of the exchange process appears to be stabilization of a nucleotide-free form of the GTPases. This, in turn decreases the affinity of the GEF–GTPase complex for nucleotides through an increase in nucleotide dissociation rate. GTPase loading can then rapidly equilibrate to a composition that depends on the intrinsic affinities for GTP and GDP (which varies appreciably among the Ras superfamily members) and local cellular concentrations of the two nucleotides[27,59]. Recent structures of the Ras–SOS[49] and Arf–Gea2[60] complexes have illustrated that the mechanics underlying these thermodynamic changes are complex. In both cases, recognition occurs through extensive contacts centered on the switch II region of the GTPase and extending to switch I and the α3 helix. Switch regions I and II are extensively rearranged on complexation, opening the nucleotide pocket dramatically. Nucleotide and Mg^{2+} binding sites are also disrupted either through direct insertion of GEF residues, conformational changes in specific GTPase side chains, or both. It is not clear which of the interactions with GEF drive the conformational changes, and therefore drive catalysis, and which simply result from optimization of energetics in the nucleotide-free, distorted state. For the SEC7 domain, approximately 10^3 of the total 10^5-fold increase in nucleotide dissociation rate can be attributed to insertion of a single Glu side chain into the nucleotide phosphate binding pocket[60,61]. In the case of SOS, however, it appears from sequence alignments that the interactions may be distributed, with no single residue being absolutely essential to the process[49]. Dbl family sequence variability may then reflect a similar situation in DH-mediated GEF catalysis.

Mutagenesis studies indicate that mechanisms of DH action may also be significantly different from those observed for SOS and Gea2[62]. Thus sensitivity of Rho and Cdc42 toward Lbc and Cdc24 respectively, is unaffected by extensive mutations throughout the switch II regions. In contrast, mutations in switch I significantly decrease GEF responsiveness. Moreover, individual mutations in switch I have different effects on responsiveness to different GEFs. For example Rho mutations T35A and F39E abrogate GEF activity of Lbc, but do not effect that of Dbl[62]. Thus, it appears that DH catalyzed exchange may have certain characteristics that are mechanistically distinct from those of other GEFs, and that even within the family there may be more subtle differences in recognition. The observed variability in DH sequence

could then also reflect these issues. Because of these complexities of DH-mediated exchange catalysis, complete understanding of Dbl family GEF activity will require structures of at least several family members both free and in complex with their GTPase substrates. The work described here provides a first step in this direction, and establishes a foundation for further study of the biochemical and biological functions of the Dbl proteins.

Note added in proof: While this manuscript was under review the structures of the DH-PH tandem from SOS[63] and the N-terminal DH domain of Trio[64] were reported. Both structures are very similar to the one described here.

Methods

NMR sample preparation. Residues 82–289 (DH domain construct) or 82–406 (DH-PH tandem construct) of βPIX were amplified from the full-length cDNA by PCR, subcloned into the pET11a expression vector (Novagen) and transformed into *E.coli* strain BL21(DE3). Uniform ^{15}N and ^{13}C labeling was obtained by growing cells in minimal media supplemented with $^{15}NH_4Cl$ and/or $^{13}C_6$-glucose as the sole nitrogen and carbon sources respectively. Random fractional deuteration was obtained by growing cells in media containing 50–75% D_2O. Full deuteration at all proton positions was obtained by growing cells in 100% D_2O media supplemented with $^{13}C_6{}^2H_7$-glucose (Cambridge Isotope Laboratories) as the sole carbon source. Selective protonation at methyl positions of leucine, valine and isoleucine was obtained as described[35] by addition of 60 mg l^{-1} of $^{13}C,^{15}N,2\text{-}^2H$ (50%),3-^2H valine (Cambridge Isotope Laboratories) and ~40 mg l^{-1} $^{13}C,3\text{-}^2H_2$ α-ketobutyrate to fully deuterated media 30 min before induction. Similarly, addition of 50 mg l^{-1} unlabeled protonated tyrosine and phenylalanine led to the protonation of the side chains of these aromatics. Cells were grown at 37 °C to an optical density of 0.8 at 600 nm. Protein expression was induced for 12 h with 1 mM isopropyl-D-thiogalactoside at 25 °C (H_2O and partially deuterated growths) or 30 °C (100% deuterated media). Protein was purified from bacterial lysate by successive weak anion exchange (Pharmacia DEAE-CL6B), strong anion exchange (Pharmacia Mono-Q) and gel filtration (Pharmacia Superdex-75) chromatographies. NMR samples contained approximately 1.3 mM protein in 20 mM phosphate buffer pH 7, 150 mM NaCl, 1 mM EDTA, 3 mM DTT, 0.1% NaN_3.

Dbl and UNC-73 mutagenesis and protein expression. Wild type and mutant cDNAs (generated by PCR and verified by automated sequencing in both directions) encoding the DH and PH domains of Dbl (residues 498–825) were fused to a cDNA encoding glutathione S-transferase (GST) and inserted into the baculovirus transfer vector pVL1393 (Invitrogen). Recombinant baculovirus was produced by transfection into Sf9 insect cells using the BaculoGold kit (Pharmingen). Expression and purification of GST-fusion small GTP-binding proteins in *E. coli* and the GST-fusion Dbl mutants in Sf9 cells were performed as described[65]. Expression and purification of UNC-73 proteins spanning residues 1179–1638 (DH-1/PH-1/SH3) were as described[23].

Nucleotide exchange assays. In assays of UNC-73, 2 μg of GST-Rac was preloaded with ^3H-GDP, then mixed in reaction buffer with 0.5 μg of the exchange factor. The amount of ^3H-GDP bound to Rac at time point 0 min was used to determine 100% GDP-bound. Dbl-induced ^3H-GDP/GTP exchange on Cdc42Hs and RhoA was measured at 24 °C as described[65] using ~0.5 μg purified GST-Dbl mutants and 1 μg GTPase.

NMR spectroscopy. NMR experiments were carried out at 38 °C on a Varian Innova 600 MHz spectrometer equipped with four channels and pulsed field gradients. Data were processed using NMRpipe[66] and analyzed with NMRview software packages[67]. Backbone ^1HN, ^{15}N, $^{13}C\alpha$, $^{13}C\beta$ and ^{13}CO assignments were obtained for the DH domain through the following ^2H-decoupled, triple resonance spectra applied to a $^2H(75\%)/^{15}N/^{13}C$-labeled sample: CT-HNCa, CT-HN(CO)Ca, HN(Ca)Cb, HN(COCa)Cb[68], HNCO[69–71] and HN(Ca)CO[72]. Assignments were confirmed by HNCaHa[69,73] and Ha(CaCO)NNH[69,74] spectra acquired on a fully protonated $^{15}N/^{13}C$-labeled sample, and through sequential HN-HN and HN-Ha NOEs observed in an ^{15}N-edited NOESY spectrum[75]. Side chain resonances were assigned on a fully protonated sample through HCCH-TOCSY[33], CCC-TOCSY-NNH and HCC-TOCSY-NNH[32] experiments. Some side chain ^1H and ^{13}C assignments were also obtained through the latter experiment applied to a $^2H(75\%)/^{15}N/^{13}C$-labeled sample. All leucine, valine and isoleucine (δ) methyl ^1H and ^{13}C assignments were obtained using the selectively methyl/aromatic protonated sample described in the text using optimized versions of the HCC- and CCC-TOCSY-NNH experiments[39]. All Phe and Tyr aromatic proton assignments were obtained through homonuclear ^1H-^1H TOCSY and NOESY experiments applied to the same sample.

The following NOESY spectra were used to generate distance restraints for structure calculation: 3D ^{15}N-edited NOESY (40 ms, 70 ms; ^{15}N-labeled sample); 3D ^{13}C-edited NOESY, 3D simultaneous $^{15}N/^{13}C$-edited NOESY (both 75 ms; $^{15}N/^{13}C$-labeled sample); 3D constant time ^{13}C-edited NOESY (175 ms), 2D ^1H NOESY (175 ms), 4D $^{13}C/^{13}C$ edited NOESY (175 ms) and 4D $^{13}C/^{15}N$ edited NOESY (175 ms mixing time) all recorded on the selectively methyl/aromatic protonated sample.

A total of 38 χ1 (±20–40°) and 14 χ2 dihedral restraints (±40°, Leu residues only) were identified based on patterns of intraresidue and sequential NOEs in the ^{15}N- and ^{13}C-edited NOESY spectra. Stereospecific Hβ assignments for 11 Leu residues were obtained similarly. Stereospecific assignments of valine and leucine methyl groups were obtained from a CT-$^1H/^{13}C$ HSQC spectrum of a 10% ^{13}C-labeled sample[76].

Structure calculations. Initial structures were calculated using a standard torsion angle simulated annealing dynamics protocol implemented in the program CNS version 0.3[77]. Distance restraints in these calculations were obtained from the 3D ^{15}N-edited NOESY, 3D ^{13}C-edited NOESY, 4D $^{13}C/^{13}C$ edited NOESY, 4D $^{13}C/^{15}N$ and the 3D CT methyl edited experiments as described in the text. Restraints were classified as strong (1.8–2.7 Å, 2.9 Å for amides) medium (1.8–3.5 Å) and weak (1.8–5.0 Å). An additional 0.5 Å was added to the upper bound for all methyl groups. Helices were initially identified by analysis of the chemical shift index[42], short and medium range HN-Hα and Hα-Hβ NOEs and backbone HN exchange data. For the 116 residues that satisfied the α-helix conformation under these criteria, φ and ψ dihedral restraints of -60° ± 30° and -40° ± 50° respectively, were included. Converged structures from the CNS calculations were then used as input to ARIA[43], which was subsequently utilized for the iterative automated assignment of all spectra and refinement of the structures using X-PLOR (version 3.851)[78]. Tolerances for the automated assignment of NOE peaks in ARIA were set to 0.04 p.p.m. in indirect and acquisition proton and 0.4 p.p.m. in heteroatom dimension for all spectra. Peaks in severely overlapped regions of the spectra were not included to avoid false assignments due to incorrect positioning of these peaks. Ten structures were calculated in each iteration. The iterative assignment of NOEs was based on eight structures with the lowest number of violations calculated in the preceding iteration. An assignment was included if it could be satisfied in at least 50% of the structures. The cutoff value of an ambiguous assignment was reduced progressively from 0.99 for the first iteration to 0.45 in iteration 11. After each iteration, structures obtained were analyzed to ensure that none of the restraints utilized in the initial CNS calculations were violated. Final structures were evaluated using the program ProcheckNMR[79].

Coordinates. Coordinates have been deposited in the Protein Data Bank (accession number 1BY1).

Acknowledgments

We thank Y. Min Chook and J. Goldberg for discussion and critical reading of the manuscript; J.Goldberg and S. Bagrodia and R. Cerione for communicating results prior to publication; L. Kay for generously providing many of the NMR pulse sequences used in this study; M. Clore for advice; A. Majumdar and Y. Gosser for assistance with NMR data acquisition; J. Hubbard for computer system support and S. Freihaut for expert administrative assistance. B.A. is supported by a grant from the U.S. Army Breast Cancer Program. M.K.R. gratefully acknowledges support from the National Institutes of Health (PECASE program), Arnold and Mabel Beckman Foundation and Sidney Kimmel Foundation for Cancer Research.

Received 8 October, 1998; accepted 16 October, 1998.

1. Hall, A. Rho GTPases and the actin cytoskeleton. *Science* **279**, 509–514 (1998).
2. Kozma, R., Ahmed, S., Best, A. & Lim, L. The Ras-related protein Cdc42Hs and bradykinin promote formation of peripheral actin microspikes and filopodia in Swiss 3T3 fibroblasts. *Mol. Cell Biol* **15**, 1942–1952 (1995).
3. Nobes, C. D. & Hall, A. Rho, rac, and cdc42 GTPases regulate the assembly of multimolecular focal complexes associated with actin stress fibers, lamellipodia, and filopodia. *Cell* **81**, 53–62 (1995).
4. Ridley, A. J., Paterson, H. F., Johnstone, C. L., Diekmann, D. & Hall, A. The small GTP-sinding protein rac regulates growth factor-induced membrane ruffling. *Cell* **70**, 401–410 (1992).
5. Ridley, A. J. & Hall, A. The small GTP-binding protein rho regulates the assembly of focal adhesions and actin stress fibres in response to growth factors. *Cell* **70**, 389–399 (1992).
6. Olson, M. F., Ashworth, A. & Hall, A. An essential role for Rho, Rac, and Cdc42 GTPases in cell cycle progression through G1. *Science* **269**, 1270–1272 (1995).
7. Minden, A., Lin, A., Claret, F. X., Abo, A. & Karin, M. Selective activation of the JNK signaling cascade and c-Jun transcriptional activity by the small GTPases Rac and Cdc42Hs. *Cell* **81**, 1147–1157 (1995).
8. Coso, O.A. *et al.* The small GTP-binding proteins Rac1 and Cdc42 regulate the activity of the JNK/SAPK signaling pathway. *Cell* **81**, 1137–1146 (1995).
9. Bagrodia, S., Derijard, B., Davis, R. J. & Cerione, R. A. Cdc42 and PAK-mediated signaling leads to Jun kinase and p38 mitogen- activated protein kinase activation. *J. Biol. Chem.* **270**, 27995–27998 (1995).
10. Hill, C. S., Wynne, J. & Treisman, R. The Rho family GTPases RhoA, Rac1, and CDC42Hs regulate transcriptional activation by SRF. *Cell* **81**, 1159–1170 (1995).
11. Qiu, R. G., Chen, J., Kirn, D., McCormick, F. & Symons, M. An essential role for Rac in Ras transformation. *Nature* **374**, 457–459 (1995).
12. Michiels, F., Habets, G. G., Stam, J. C., van der Kammen, R. A. & Collard, J. G. A role for Rac in Tiam1-induced membrane ruffling and invasion. *Nature* **375**, 338–340 (1995).
13. Pasteris, N. G. *et al.* Isolation and characterization of the faciogenital dysplasia (Aarskog-Scott syndrome) gene: a putative Rho/Rac guanine nucleotide exchange factor. *Cell* **79**, 669–678 (1994).
14. Billuart, P. *et al.* Oligophrenin-1 encodes a rhoGAP protein involved in X-linked mental retardation. *Nature* **392**, 923–926 (1998).
15. Bourne, H. R., Sanders, D. A. & McCormick, F. The GTPase superfamily: a conserved switch for diverse cell functions. *Nature* **348**, 125–131 (1990).
16. Bokoch, G. M. & Der, C. J. Emerging concepts in the Ras superfamily of GTP-binding proteins. *FASEB J.* **7**, 750–759 (1993).
17. Boguski, M. & McCormick, F. Proteins regulating Ras and its relatives. *Nature* **366**, 643–654 (1993).
18. Cerione, R. A. & Zheng, Y. The Dbl family of oncogenes. *Curr Opin Cell Biol* **8**, 216–222 (1996).
19. Zheng, Y., Zangrilli, D., Cerione, R. A. & Eva, A. The pleckstrin homology domain mediates transformation by oncogenic dbl through specific intracellular targeting. *J Biol Chem* **271**, 19017–19020 (1996).
20. Hart, M. J. *et al.* Cellular transformation and guanine nucleotide exchange activity are catalyzed by a common domain on the dbl oncogene product. *J. Biol. Chem.* **269**, 62–65 (1994).
21. Chuang, T. H. *et al.* Abr and Bcr are multifunctional regulators of the Rho GTP-binding protein family. *Proc. Natl. Acad. Sci. USA* **92**, 10282–10286 (1995).
22. Zheng, Y. *et al.* The faciogenital dysplasia gene product FGD1 functions as a Cdc42Hs- specific guanine-nucleotide exchange factor. *J. Biol. Chem.* **271**, 33169–33172 (1996).
23. Steven, R. *et al.* UNC-73 activates the Rac GTPase and is required for cell and growth cone migrations in *C. elegans*. *Cell* **92**, 785–795 (1998).
24. Horii, Y., Beeler, J. F., Sakaguchi, K., Tachibana, M. & Miki, T. A novel oncogene, ost, encodes a guanine nucleotide exchange factor that potentially links Rho and Rac signaling pathways. *EMBO J.* **13**, 4776–4786 (1994).
25. Miki, T., Smith, C. L., Long, J. E., Eva, A. & Fleming, T. P. Oncogene ect2 is related to regulators of small GTP-binding proteins [published erratum appears in *Nature* **364**, 737]. *Nature* **362**, 462–465 (1993).
26. Glaven, J. A., Whitehead, I. P., Nomanbhoy, T., Kay, R. & Cerione, R. A. Lfc and Lsc oncoproteins represent two new guanine nucleotide exchange factors for the Rho GTP-binding protein. *J Biol Chem* **271**, 27374–27381 (1996).
27. Klebe, C., Prinz, H., Wittinghofer, A. & Goody, R. S. The kinetic mechanism of Ran-nucleotide exchange catalyzed by RCC1. *Biochemistry* **34**, 12543–12552 (1995).
28. Pawson, T. Protein modules and signalling networks. *Nature* **373**, 573–580 (1995).
29. Musacchio, A., Gibson, T., Rice, P., Thompson, J. & Saraste, M. The PH domain: a common piece in the structural patchwork of signalling proteins. *Trends Biochem. Sci.* **18**, 343–348 (1993).
30. Bagrodia, S., Taylor, S. J., Jordon, K. A., Van Aelst, L. & Cerione, R. A. A novel regulator of p21-activated kinases. *J. Biol. Chem.* **273**, 23633–23636 (1998).
31. Manser, E. *et al.* PAK kinases are directly coupled to the PIX family of nucleotide exchange factors. *Mol. Cell* **1**, 183–192 (1998).
32. Logan, T. M., Olejniczak, E. T., Xu, R. X. & Fesik, S. W. A general method for assigning NMR spectra of denatured proteins using 3D HC(CO)NH-TOCSY triple resonance experiments. *J. Biomol. NMR* **3**, 225–231 (1993).
33. Kay, L. E., Xu, G. Y., Singer, A. U., Muhandiram, D. R. & Forman-Kay, J. D. A gradient-enhanced HCCH-TOCSY experiment for recording side-chain proton and carbon-13 correlations in water samples of proteins. *J. Magn. Reson. Ser. B* **101**, 333–337 (1993).
34. Rosen, M. *et al.* Selective methyl group protonation of perdeuterated proteins. *J. Mol. Biol.* **263**, 627–636 (1996).
35. Gardner, K. & Kay, L. Production and incorporation of ^{15}N, ^{13}C, $^{2}H(^{1}H$-1 methyl) isoleucine into proteins for multidimensional NMR studies. *J. Am. Chem. Soc.* **119**, 7599–7600 (1997).
36. Gardner, K., Rosen, M. & Kay, L. Global folds of highly deuterated, methyl potonated proteins by multidimensional NMR. *Biochemistry* **36**, 1389–1401 (1997).
37. Metzler, W., Whittekind, M., Goldfarb, V., Mueller, L. & Farmer, B. Incorporation of $^{1}H/^{13}C/^{15}N$-(Ile, Leu, Val) into perdeuterated, ^{15}N-labeled protein: potential in structure determination of large proteins by NMR. *J. Am. Chem. Soc.* **118**, 6800–6801 (1996).
38. Smith, B. *et al.* An approach to global fold determination using limited NMR data from larger proteins selectively protonated at specific residues. *J. Biomol. NMR* **8**, 360–368 (1996).
39. Gardner, K., Konrat, R., Rosen, M. & Kay, L. A (H)C(CO)NH-TOCSY pulse scheme for sequential assignment of protonated methyl groups in otherwise deuterated ^{15}N, ^{13}C labeled proteins. *J. Biomol. NMR* **8**, 351–356 (1996).
40. Wuthrich, K. *NMR of proteins and nucleic acids* (John Wiley & Sons, New York; 1986).
41. Zwahlen, C., Vincent, S. J. F., Gardner, K. H. & Kay, L. E. Significantly improved resolution for NOE correlations from valine and isoleucine (Cg2) methyl groups in $^{15}N,^{13}C$- and ^{15}N, ^{13}C, ^{2}H-labeled proteins. *J. Am. Chem. Soc.* **120**, 4825–4831 (1998).
42. Wishart, D. S. & Sykes, B. D. The ^{13}C chemical-shift index: a simple method for the identification of protein secondary structure using ^{13}C chemical-shift data. *J. Biomol. NMR* **4**, 171–180 (1994).
43. Nilges, M., Macias, M. J., O'Donoghue, S. I. & Oschkinat, H. Automated NOESY interpretation with ambiguous distance restraints: the refined NMR solution structure of the pleckstrin homology domain from beta-spectrin. *J. Mol. Biol.* **269**, 408–422 (1997).
44. Holm, L. & Sander, C. Protein structure comparison by alignment of distance matrices. *J. Mol. Biol.* **233**, 123–138 (1993).
45. Yu, H. & Schreiber, S. L. Structure of guanine-nucleotide-exchange factor human Mss4 and identification of its Rab-interacting surface. *Nature* **376**, 788–791 (1995).
46. Mossessova, E., Gulbis, J. M. & Goldberg, J. Structure of the guanine nucleotdie exchange factor of human ARNO and analysis of the interaction with ARF GTPase. *Cell* **92**, 415–423 (1998).
47. Cherfils, J. *et al.* Structure of the Sec7 domain of the Arf exchange factor ARNO. *Nature* **392**, 101–104 (1998).
48. Renoult, L. *et al.* The 1.7 A crystal structure of the regulator of chromosome condensation (RCC1) reveals a seven-bladed propeller. *Nature* **392**, 97–101 (1998).
49. Boriack-Sjodin, P. A., Margarit, S. M., Bar-Sagi, D. & Kuriyan, J. The structural basis of the activation of Ras by SOS. *Nature* **394**, 337–343 (1998).
50. Pervushin, K., Riek, R., Wider, G. & Wuthrich, K. Attenuated T2 relaxation by mutual cancellation of dipole-dipole coupling and chemical shift anisotropy indicates an avenue to NMR structures of very large biological macromolecules in solution. *Proc. Natl. Acad. Sci. USA* **94**, 12366–12371 (1997).
51. Crespo, P. *et al.* Rac1 dependent stimulation of the JNK/SAPK signaling pathway by Vav. *Oncogene* **13**, 455–462 (1996).
52. Miyamoto, S. *et al.* A DBL-homologous region of the yeast CLS4/CDC24 gene product is important for Ca(2+)-modulated bud assembly. *Biochem. Biophys. Res. Comm.* **181**, 604–610 (1991).
53. Ron, D. *et al. New Biologist* **3**, 372–379 (1991).
54. Zheng, J. *et al.* The solution structure of the pleckstrin homology domain of human SOS1. *J. Biol. Chem.* **272**, 30340–30344 (1997).
55. Koshiba, S. *et al.* The solution structure of the pleckstrin homology domain of mouse son-of-sevenless 1 (mSos1). *J. Mol. Biol.* **269**, 579–591 (1997).
56. Nimnual, A. S., Yatsula, B. A. & Bar-Sagi, D. Coupling of Ras and Rac guanosine triphosphatases through the Ras exchanger Sos. *Science* **279**, 560–563 (1998).
57. Olson, M. F., Sterpetti, P., Nagata, K., Toksoz, D. & Hall, A. Distinct roles for DH and PH domains in the Lbc oncogene. *Oncogene* **15**, 2827–2831 (1997).
58. Whitehead, I., Kirk, H., Tognon, C., Trigo-Gonzalez, G. & Kay, R. Expression cloning of lfc, a novel oncogene with structural similarities to guanine nucleotide exchange factors and to the regulatory region of protein kinase C. *J. Biol. Chem.* **270**, 18388–18395 (1995).
59. Lenzen, C., Cool, R. H., Prinz, H., Kuhlmann, J. & Wittinghofer, A. Kinetic analysis by fluorescence of the interaction between Ras and the catalytic domain of the guanine nucleotide exchange factor Cdc25Mm. *Biochemistry* **37**, 7420–7430 (1998).
60. Goldberg, J. Structural basis for activation of ARF GTPase: Mechanisms of guanine nucleotide exchange and GTP-myristoyl switching. *Cell*, **95**, 273–248 (1998).
61. Beraud-Dufour, S. *et al.* A glutamic finger in the guanine nucleotide exchange factor ARNO displaces Mg2+ and the beta-phosphate to destabilize GDP on ARF1. *EMBO J.* **17**, 3651–3659 (1998).
62. Li, R. & Zheng, Y. Residues of the Rho family GTPases Rho and Cdc42 that specify sensitivity to Dbl-like guanine nucleotide exchange factors. *J. Biol. Chem.* **272**, 4671–4679 (1997).
63. Soisson, S. M., Nimnual, A. S., Uy, M., Bar-Sagi, D. & Kuriyan, J. Crystal structure of the Dbl and pleckstrin homology domains from the human son of sevenless protein. *Cell* **95**, 259–268 (1998).
64. Liu, X. *et al.* NMR structure and mutagenesis of the N-terminal Dbl homology domain of the nucleotide exchange factor trio. *Cell* **95**, 269–277 (1998).
65. Zheng, Y., Cerione, R. & Bender, A. Control of the yeast bud-site assembly GTPase Cdc42. Catalysis of guanine nucleotide exchange by Cdc24 and stimulation of GTPase activity by Bem3. *J. Biol. Chem.* **269**, 2369–2372 (1994).
66. Delaglio, F. *et al.* NMRPipe: a multidimensional spectral processing system based on UNIX pipes. *J. Biomol. NMR* **6**, 277–293 (1995).
67. Johnson, B. A. & Blevins, R. A. NMR View: a computer program for the visualization and analysis of NMR data. *J. Biomol. NMR* **4**, 603–614 (1994).
68. Yamazaki, T., Lee, W., Aerosmith, C., Muhandiriam, D. & Kay, L. A suite of tiple resonance NMR experiments for the backbone assignment of ^{15}N, ^{13}C, ^{2}H labeled proteins with high sensitivity. *J. Am. Chem. Soc.* **116**, 11655–11666 (1994).
69. Muhandiram, D. R. & Kay, L. E. Gradient-enhanced triple-resonance three-dimensional NMR experiments with improved sensitivity. *J. Magn. Reson. Ser. B* **103**, 203–216 (1994).
70. Kay, L. E., Y., X. G. & Yamazaki, T. Enhanced-sensitivity triple-resonance spectroscopy with minimal H_2O Saturation. *J. Magn. Reson. Ser. A* **109**, 129–133 (1994).
71. Kay, L. E., Ikura, M., Tschudin, R. & Bax, A. Three dimensional triple-resonance NMR spectroscopy of isotopically enriched proteins. *J. Magn. Reson.* **89**, 496–514 (1990).

72. Matsuo, H., Kupce, E., Li, H. & Wagner, G. Use of Selective C alpha pulses for improvement of HN(CA)CO-D and HN(COCA)NH-D experiments. *J. Magn. Reson. Ser. B* **111**, 194–198 (1996).
73. Clubb, R. T., Thanabal, V. & Wagner, G. A new 3D HN(CA)HA experiment for obtaining fingerprint H^N -H^a cross peaks in ^{15}N- and ^{13}C-labeled proteins. *J. Biomol. NMR* **2**, 203–210 (1992).
74. Grzesiek, S. & Bax, A. Correlating backbone amide and side chain resonances in larger proteins by multiple relayed triple resonance NMR. *J. Am. Chem. Soc.* **114**, 6291–6293 (1992).
75. Palmer, A. G. I., Cavanagh, J., Byrd, R. A. & Rance, M. Sensitivity improvement in three-dimensional heteronuclear correlation NMR spectroscopy. *J. Magn. Reson.* **96**, 416–424 (1992).
76. Neri, D., Szyperski, T., Otting, G., Senn, H. & Wuthrich, K. Stereospecific nuclear magnetic resonance assignments of the methyl groups of valine and leucine in the DNA-binding domain of the 434 repressor by biosynthetically directed fractional ^{13}C labeling. *Biochemistry* **28**, 7510–7516 (1989).
77. Brunger, A. T. Crystallography and NMR system. *Acta Crystallogr.* **D54**, 905–921 (1998).
78. Brünger, A. T. *X-PLOR manual* (Yale University, New Haven, Connecticut; 1993).
79. Laskowski, R. A., Rullmannn, J. A., MacArthur, M. W., Kaptein, R. & Thornton, J. M. AQUA and PROCHECK-NMR: programs for checking the quality of protein structures solved by NMR. *J. Biomol. NMR* **8**, 477–486 (1996).
80. Carson, M. J. Ribbons 2.0. *J. Appl. Crystallogr.* **24**, 958–961 (1991).
81. Nicholls, A., Sharp, K. A. & Honig, B. Protein folding and association: insights from the interfacial and thermodynamic properties of hydrocarbons. *Struct. Funct. Genet.* **11**, 281–296 (1991).

product review

Oxford Cryosystems has announced the launch of the Oxford HeliX, the first commercially available helium system for X-ray crystallography in which the crystal sample is cooled in an open flow gas stream rather than being enclosed by windows. The Oxford HeliX utilizes helium gas, not liquid, from a helium cylinder and cools it to temperatures as low as 28 K. This is achieved by using a integrated two stage closed cycle cooler and a patented gas delivery system. Other benefits of the Oxford HeliX include: temperature stability of 0.3 K, reduction of helium gas consumption to 7.5 l min^{-1}, a push button temperature controller that is simple to use, and proven mechanical reliability. The low flow rate is designed to minimize the consumption of helium while still providing sufficient flow to cool the sample and eliminate the possibility of ice formation.

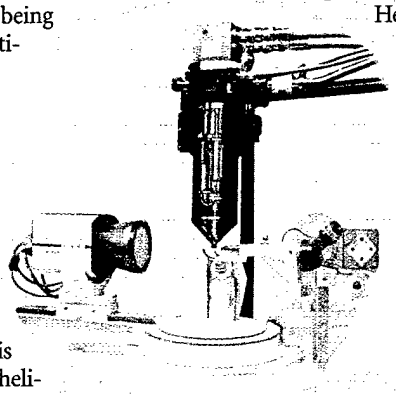

Oxford Cryosystems is the home of the nitrogen gas Cryostream Cooler, a popular flow nitrogen system. The design of that system has helped to make the difficult task of low temperature X-ray data collection a more routine procedure, and now the development of the Oxford HeliX will allow routine data collection at even lower temperatures.

The Oxford HeliX is useful for any crystallographer wishing to collect X-ray data below nitrogen temperatures where an open flow gas stream is essential. Experiments in which this would be useful include charge density studies, where lower temperatures offer enhanced data quality, and the cooling of biological samples in intense X-ray sources, where lower temperatures can increase the life time of the crystal.

For more information on the Oxford HeliX, contact:
Oxford Cryosystems
www.OxfordCryosystems.co.uk
email: info@OxfordCryosystems.co.uk

Molecular Structure Corporation has developed the first commercially available xenon derivatization flash cooling device, the Cryo-Xe-Siter. A critical step in X-ray crystallographic structure determination of a macromolecule is the preparation of heavy atom derivatives of the crystal. The noble gas xenon binds to hydrophobic sites and can serve as the needed heavy atom derivative. However, a major challenge to the widespread use of xenon has been the technical difficulty of preparing the derivatized crystals. Now, with the the Cryo-Xe-Siter, xenon derivatives of protein crystals can be produced easily — and at cryogenic temperatures.

The unique two-chamber design allows a protein crystal to reach equilibrium in the xenon atmosphere, at pressures up to 300 p.s.i. The crystal is then flash frozen while still under pressure. The Cryo-Xe-Siter accommodates popular pin mounts and has a small chamber to minimize xenon consumption. It is easy to use and safe to operate.

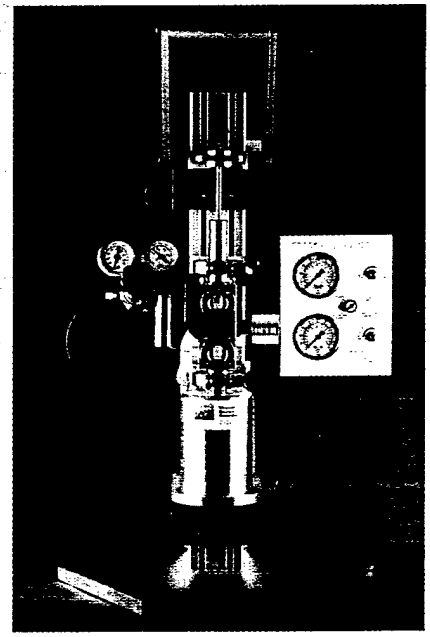

For more information on the Cryo-Xe-Siter, contact:
Molecular Structure Corporation
tel. 281 363 1033
fax 281 364 3628
http://www.msc.com/